SUPPORTING INFORMATION

Spatial Atmospheric Pressure Molecular Layer Deposition of Alucone films using Dimethylaluminum Isopropoxide as Precursor

Hardik Jain[a,b], *Mariadriana Creatore*[b], *Paul Poodt*[a,b]*

[a]TNO/Holst Centre, 5656 AE Eindhoven, Netherlands

[b]Department of Applied Physics, Eindhoven University of Technology, 5600 MB Eindhoven, The Netherlands

(*paul.poodt@tno.nl)

Contents

A. Ex-situ X-ray photoelectron spectroscopy

X-ray photoelectron spectroscopy was employed to acquire survey spectra of the top part of the as-prepared alucone films (using DMAI and TMA). The respective spectra are shown in Figure S1. It can be observed that both the spectra are dominated by three peaks corresponding to Al 2p, C 1s and O 1s all of which are expected in an alucone film. The relative elemental compositions of the three elements as determined using the respective areas of their peaks are also shown in Table S1. It must, however, be kept in mind that the films were momentarily exposed to the ambient environment while they were transferred from the deposition setup to the XPS tool and thus, survey spectra acquired from the top part of the films might not best reflect the original composition of the films.

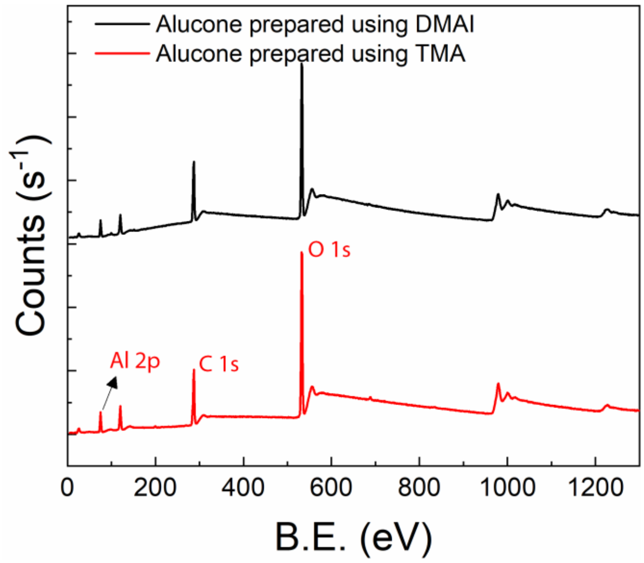

Element	Relative composition	
	DMAI	TMA
Al	14.7	17.8
C	43.1	36.6
O	42.1	45.6

Figure S1: Survey spectra of the top part of the as-prepared alucone films employing DMAI (black) and TMA (red). Table S1: Relative elemental composition of the films as revealed by the survey spectra of their top surfaces

To overcome the problem of ambient exposure, high-resolution spectra of Al 2p, C 1s and O 1s were acquired from both films after 8 cycles of ion sputtering and compared (Figure S2). The binding energies were referenced to the adventitious C 1s peak at 284.8 eV to correct for any shifts. The corrected spectra and the peaks used to simulate each of the elemental environments are displayed in Figure S*2* and Table S2.

DMAI + EG alucone film

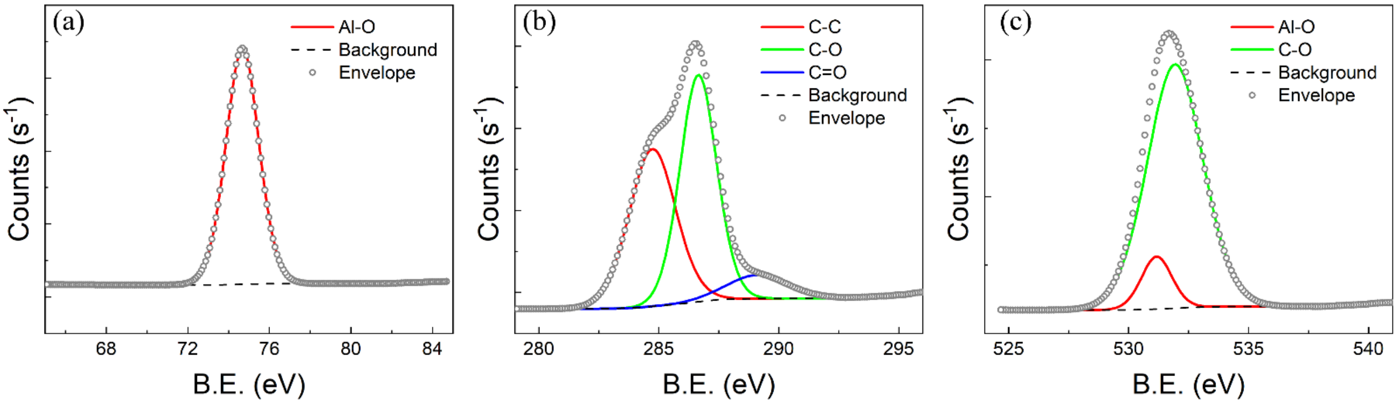

TMA + EG alucone film

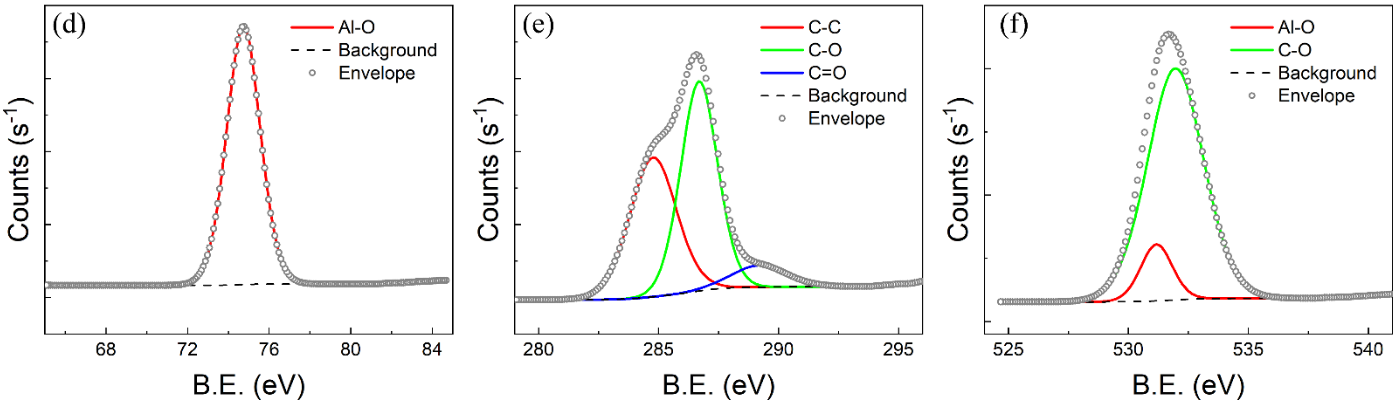

Figure S2: High-resolution spectra of Al 2p (a,d), C 1s (b,e) and O 1s (c,f) as acquired from alucone films prepared using DMAI (top row) and TMA (bottom row) as metal precursors

Table S2: Relative elemental composition of the films after 8 ion sputtering cycles and the positions of the fitted peaks

Element	Relative elemental composition (%)		Fitted peak positions (eV)	
	DMAI	TMA	DMAI	TMA
Al	23	24	74.8 (Al-O)	74.8 (Al-O)
C	53	53	284.8 (C-C) 286.85 (C-O) 289.1 (C=O)	284.8 (C-C) 286.9 (C-O) 289.0 (C=O)
O	24	23	531.2 (Al-O) 531.9(C-O)	531.2 (Al-O) 531.9 (C-O)

B. Degradation of the films upon ambient exposure

FTIR spectroscopy was used to monitor the changes occurring within the alucone films upon their ambient exposure. For the sake of comparison, films prepared using both of the aluminum precursors (DMAI and TMA) were monitored. At the outset, both films show relatively similar degradation behaviors as seen in Figure S3. In the low-frequency region, the peaks corresponding to Al-O phonon mode at 905 cm^{-1} altogether disappear. Also seen is that the bands corresponding to the C-O and C-C stretching vibration decrease in their intensities. In the high-frequency region, a very large absorbance band centered between 3400 - 3500 cm^{-1} appears in both of the films and corresponds to the OH stretching vibrations arising mainly from adsorbed water and changes that occur within the films upon ambient exposure[1]. Further, the bands corresponding to CH_2 vibrations in the frequency range of 2600-3000 cm^{-1} either reduce immensely in terms of their intensities or completely disappear from the spectra. The changes are also similar to those documented in the literature[1,2].

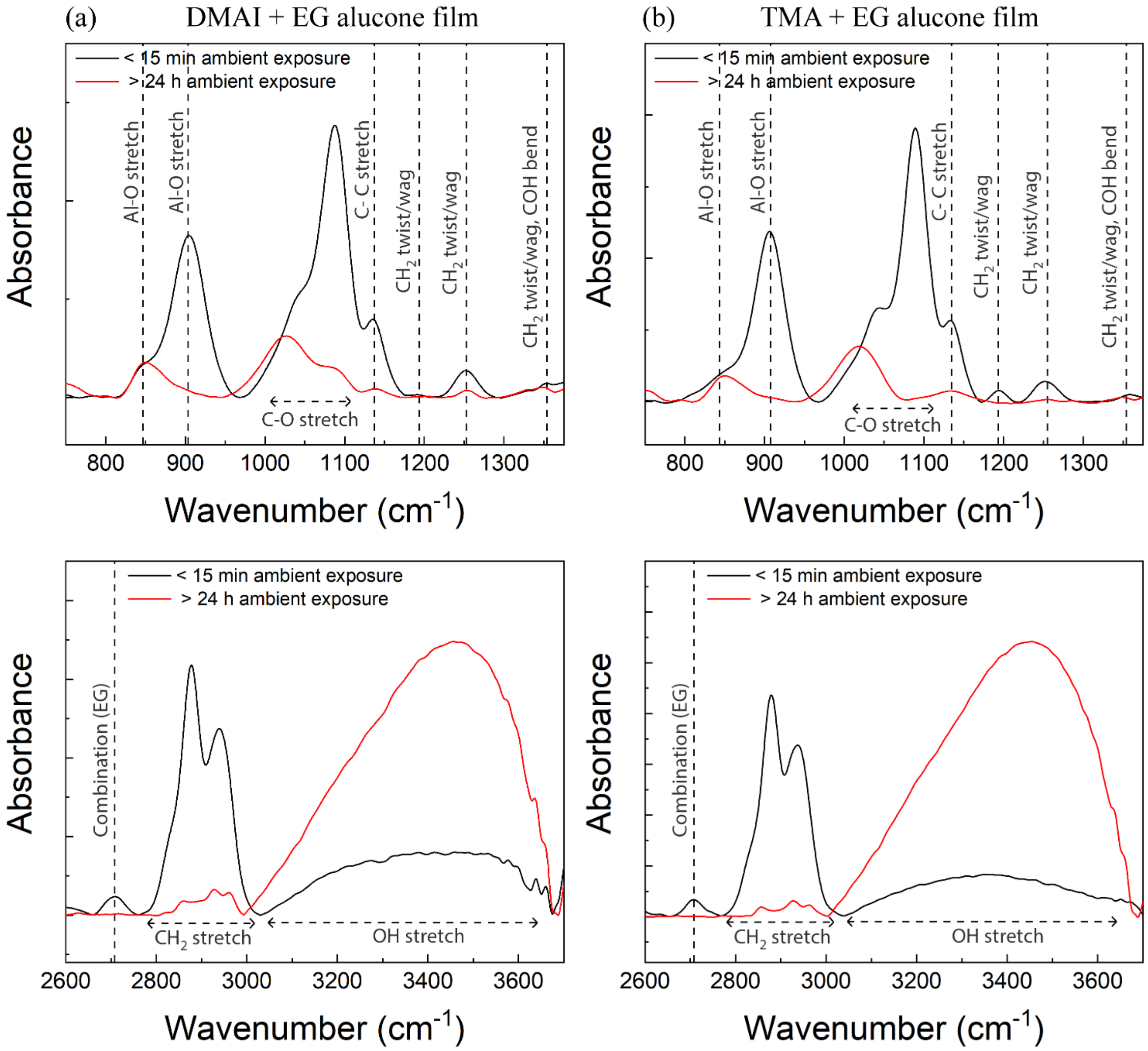

Figure S3: Changes upon ambient exposure in the FTIR spectra of alucone films prepared using a) DMAI + EG b) TMA + EG

To complement the above FTIR study, we have also monitored the changes occurring in the composition of the films using XPS analysis. Figure S4 shows the relative composition of the films after more than 24 h in ambiance and it is evident that similar changes in the relative elemental compositions of the films occur irrespective of the employed metal precursor. The relative content of oxygen in both films rises to ~ 63 percent which could be partly due to water absorption by the films. The relative aluminum content of the films was also observed to increase to ~ 29 %. On the other hand, the relative carbon content in both films reduces to a mere 7-8 %. This corresponds well to the reduction observed in the intensities of the carbon-containing bonds in the FTIR spectra above.

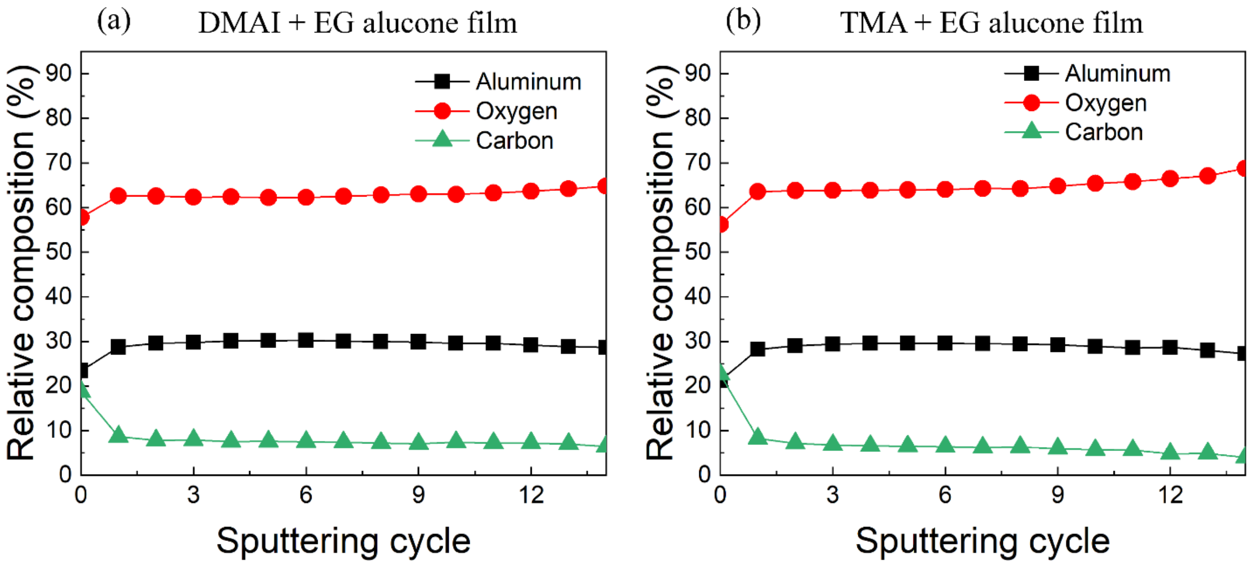

Figure S4: Relative elemental composition of air-exposed (> 24 h) alucone films deposited using a) DMAI + EG b) TMA + EG

Finally, we looked at the decrease in thickness of the DMAI + EG alucone films (Figure S5). The maximum reduction in thickness happened during the first two hours of the exposure to the ambiance. The thickness then stabilized at a value that is 74 % of its original thickness. Several factors such as handling, ambient humidity and temperature could affect the degradation but we found that the film thickness after reaching the steady-state is quite similar to what others have reported[2].

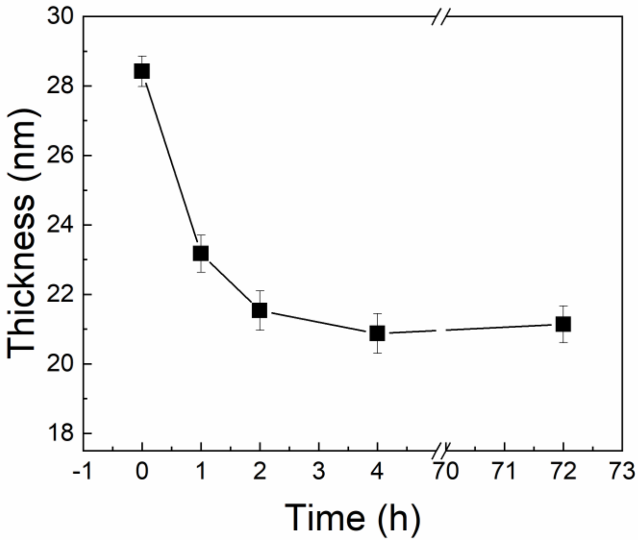

Figure S5: Change in thickness of the alucone films (DMAI + EG) with increasing ambient exposure. The thickness errors shown resulted from ellipsometry data fitting.

C. Molecular size comparison between DMAI and TMA

One of the reasons that DMAI possibly does not infiltrate into the alucone films could be its larger molecular size. Thus, we have performed simple geometric measurements of the TMA and DMAI molecules. The cross-sectional width of the TMA monomeric molecules was found to be around ~ 4 Å. On the other hand, the dimeric form of DMAI had a cross-sectional width of ~ 6.2 Å in its upright position and ~ 8.7 Å in its flat position. DMAI's larger molecular size, higher molecular weight and a different shape than TMA suggest that DMAI could indeed possess a lower diffusion coefficient[3] than TMA and thus, might find it more difficult than TMA to infiltrate into the MLD films.

References

1 A. A. Dameron, D. Seghete, B. B. Burton, S. D. Davidson, A. S. Cavanagh, J. A. Bertrand and S. M. George, *Chem. Mater.*, 2008, **20**, 3315–3326.

2 K. Van de Kerckhove, M. K. S. Barr, L. Santinacci, P. M. Vereecken, J. Dendooven and C. Detavernier, *Dalt. Trans.*, 2018, **47**, 5860–5870.

3 J. Crank, *The Mathematics of Diffusion*, Clarendon Press, Oxford, 1975.